BBA - Molecular Basis of Disease 1865 (2019) 1–13

Contents lists available at ScienceDirect

BBA - Molecular Basis of Disease

journal homepage: www.elsevier.com/locate/bbadis

mTOR inhibitor INK128 attenuates systemic lupus erythematosus by regulating inflammation-induced CD11b$^+$Gr1$^+$ cells

Guoping Shi[a], Dan Li[a], Xiaojing Li[a], Jing Ren[a], Jingjing Xu[a], Liang Ding[a], Huan Dou[a,b,*], Yayi Hou[a,b,*]

[a] The State Key Laboratory of Pharmaceutical Biotechnology, Division of Immunology, Medical School, Nanjing University, Nanjing 210093, PR China
[b] Jiangsu Key Laboratory of Molecular Medicine, Nanjing 210093, PR China

ARTICLE INFO

Keywords:
CD11b$^+$Gr1$^+$ cells
MDSCs
SLE
mTOR
Th17/Tregs balance

ABSTRACT

Systemic lupus erythematosus (SLE) is an autoimmune disease, characterized by systemic chronic inflammation that can affect multiple major organ systems. Although the etiology of SLE is known to involve a variety of factors such as the environment, random factors and genetic susceptibility, the exact role of CD11b$^+$Gr1$^+$ myeloid cells in lupus progression is not fully understood. Myeloid-derived CD11b$^+$Gr1$^+$ cells are thought to be a heterogeneous group of immature myeloid cells with immune function. Some studies have reported that CD11b$^+$Gr1$^+$ cells and the activation of mTOR pathway are involved in the pathogenesis of systemic lupus erythematosus (SLE). However, it is still not clarified about the mechanism of influence of lupus microenvironment and mTOR signaling on CD11b$^+$Gr1$^+$ cells. In the present study, we found that the percentage of CD11b$^+$Gr1$^+$ cells increased prior to the abnormal changes of Th17, Treg, T and B cells during lupus development. TLR7 and IFN-α signaling synergized to promote CD11b$^+$Gr1$^+$ cell accumulation in an mTOR-dependent manner. Moreover, compared to a traditional mTOR inhibitor, INK128 inhibited more effectively the disease activity via regulating CD11b$^+$Gr1$^+$ cell expansion and functions. Furthermore, TLR7/IFN-α-modified CD11b$^+$Gr1$^+$ cells promoted unbalance of Th17/Tregs and were inclined to differentiate into macrophages via the mTOR pathway. In conclusion, CD11b$^+$Gr1$^+$ cells increased in the early stages of the lupus progression and mTOR pathway was critical for CD11b$^+$Gr1$^+$ cells in lupus development, suggesting the changes of inflammation-induced CD11b$^+$Gr1$^+$ cells initate lupus development. We also provide evidence for the first time that INK128, a second generation mTOR inhibitor, has a good therapeutic action on lupus development by regulating CD11b$^+$Gr1$^+$ cells.

1. Introduction

Systemic lupus erythematosus (SLE) is a prototypic autoimmune disease, characterized by systemic chronic inflammation that can affect multiple major organ systems [1]. Although the etiology of SLE is known to involve a variety of factors such as the environment, random factors and genetic susceptibility, its exact pathogenesis is not fully understood [2]. Long-term dysfunction of B and T lymphocytes is considered to be the main pathological feature of SLE, so the initial study considered the role of the acquired immune system [3]. In recent years, researchers have come to realize that innate immunity may play an extremely important role in autoimmune diseases. Innate immune cells include monocytes, macrophages, dendritic cells (DCs), and neutrophils, all of which belong to myeloid cells. In autoimmune responses, myeloid cells are the key to the local and systemic immune responses of endogenous molecules released by autologous cell death, endogenous risk-signal-damage-related molecular patterns (DAMPs) [4]. Innate immune-mediated immune regulation abnormalities may be the cause of the development of SLE. Despite major advances in understanding the pathology of SLE, the role of CD11b$^+$Gr1$^+$myeloid cells changes in lupus progression is poorly understood.

Myeloid-derived suppressor cells (MDSCs) are a heterogeneous population of immature cells derived from myeloid progenitors [5]. Murine MDSCs are characterized as CD11b$^+$Gr1$^+$ cells, and can be further classified into CD11b$^+$Ly6C^{low}Ly6G$^+$ granulocytic MDSCs (G-MDSCs) and CD11b$^+$Ly6C$^+$Ly6G$^-$ monocytic MDSCs (M-MDSCs) [5,6]. Some studies have revealed that MDSCs play a crucial role in regulation of SLE, but it is still unknown on the time course changes of

* Corresponding authors at: The State Key Laboratory of Pharmaceutical Biotechnology, Division of Immunology, Medical School, Nanjing University, Nanjing 210093, PR China.
E-mail addresses: douhuan@nju.edu.cn (H. Dou), yayihou@nju.edu.cn (Y. Hou).

https://doi.org/10.1016/j.bbadis.2018.10.007
Received 11 September 2018; Accepted 2 October 2018
Available online 04 October 2018

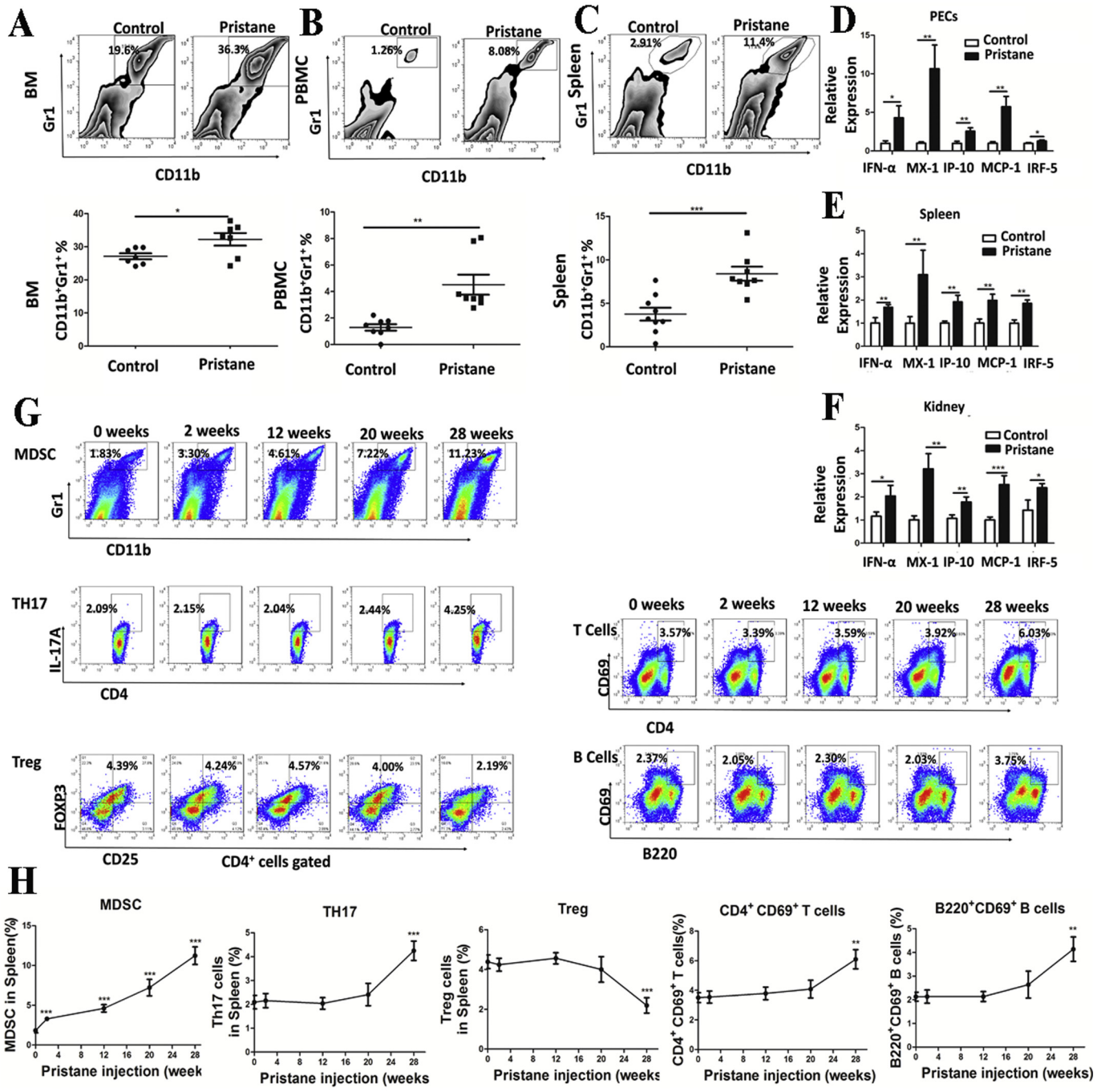

Fig. 1. The percentage of $CD11b^+Gr1^+$ cells increases in the early stages of the lupus progression. BALB/c mice (10 weeks, n = 6–8/group) were given a single intraperitoneal injection of 0.5 ml pristane or PBS and monitored for 7 months. Representative flow cytometry analyses of $CD11b^+Gr1^+$ cells in bone marrow (BM) (A), PBMC (B) and spleen (C) in control mice and pristane-induced lupus mice. Relative quantitation of *IFN-α* and *ISGs* (*MX-1*, *IP-10*, *MCP-1*, *IRF-5*) gene expressions by RT-PCR in peritoneal exudate cells (PECs) (D), spleen (E) and kidney (F) from control and lupus mice. (G–H) Kinetic changes of MDSCs, Th17, Tregs, $CD4^+CD69^+$ T cells, $B220^+CD69^+$B cells in spleen in pristane-induced lupus mice were determined by flow cytometry. Data represent the mean scores ± SEM. All experiments were repeated three times. $^*P \le 0.05$, $^{**}P \le 0.01$, $^{***}P \le 0.001$.

MDSCs and the specific regulatory mechanisms of MDSCs in SLE. Previous studies reported that laquinimod suppressed nephritis by inducing expansion of M-MDSCs and G-MDSCs in (NZB × NZW) F1 prone mice [7]. Intravenous treatment with MDSCs obtained from C57BL/6 mice induced the expansion of regulatory B cells via iNOS and ameliorated autoimmunity in $Roquin^{san/san}$ lupus mice [8]. MDSCs increased in male (NZB × NZW) F1 mice compared with female mice and directly inhibited cytokine-induced differentiation of naive B cells into antibody-secreting cells [9]. MDSCs were shown to suppress B cells differentiation in male and inhibit T cells in (NZB × NZW) F1 lupus mice, but lupus mice still developed the progressive lupus-like disease. In contrast, a study showed that the percentage of MDSCs was increased in the peripheral blood in patients with SLE compared to healthy controls. MDSCs from SLE patients promoted Th17 differentiation by an Arginase-1-dependent manner and accelerated the progress of SLE [10]. Another study showed that both impaired expansion and functional defects of G-MDSC existed in the lymphoid organs in the (NZB × NZW) F1 lupus mice with established disease. The increased elimination of G-

MDSCs was attributed to extracellular trap formation which was mediated by cytokines from the pro-inflammatory microenvironment [11]. We also found that the percentages of MDSCs were increased in SLE patients, MRL/*lpr* mice and IMQ-lupus-prone mice [12,13]. In our previous, we found MDSCs induce podocyte injury through increasing ROS in lupus nephritis [14]. G-MDSCs from diseased MRL/*lpr* mice impaired Treg differentiation via ROS, while M-MDSCs promoted Th17 cell polarization by IL-1β [13]. These data suggested that changes in both percentage and function of MDSCs may be crucial for SLE development. However, to date, it is still not clarified, which factors influence the changes of MDSCs in lupus microenvironment.

In lupus microenvironment, endogenous nucleic acids are released from apoptotic or necrotic cells and stimulate innate and adaptive immune systems to accelerate the pathologic process [15]. The recognition of self nucleic acids by TLR7 on B cells and pDCs is thought to be an important step in generating anti-nuclear antibodies and producing IFN-α [15]. It was reported that the elevated level of IFN-α is a driving pathogenic force for most SLE patients [16–20]. Moreover, the mammalian target of rapamycin (mTOR) pathway is well recognized to control cell survival, metabolism and proliferation [21]. Activation of the mTOR pathway contributes to the pathogenesis of SLE [22,23] and mTOR activation and therapeutic reversal were detected in T cells in SLE [24–28]. The roles of mTOR were also found in B cells [29], mesenchymal stem cells (MSCs) [30] and hepatocytes [31] in SLE. Of note, recent studies reported that mTOR signaling play critical roles in myeloid expansion during infection-induced myelopoiesis [32,33]. However, it is still unknown about the detailed role of mTOR on TLR7 and/or type I IFN-induced MDSCs during progressive course of SLE. Strikingly, mTOR inhibitor INK128 is an orally bioavailable, highly potent and selective adenosine triphosphate competitor of both mTORC1 and mTORC2. Currently, INK128 is in phase I and II clinical trials in patients with malignancies [34]. We hypothesize that INK128 may regulate $CD11b^+Gr1^+$ cells to achieve a therapeutic effect on SLE.

To clarify the role of mTOR on TLR7 and/or type I IFN-induced $CD11b^+Gr1^+$ cells during progressive course of SLE and determine therapeutic effect of INK128 on SLE, pristane-induced lupus mice model were applied in this study. It is reported that pristane-induced lupus mouse model can display many key immunological and clinical features of human SLE as well as high “interferon signature” levels in serum [35,36]. Pristane-induced lupus mice model was suitable to explore the role of $CD11b^+Gr1^+$ cells in lupus development. Although a study reported $CD11b^+Ly6C^{hi}$ cells have an immunosupresive role after pristane injection for 2 weeks [37], it is not -clear whether the microenvironment can change the functions of the cells since pristane-induced lupus is a long term progress. To confirm our results, MRL/lpr lupus mouse model was used [38]. The lupus model also develops many classical SLE-like features, including increased levels of immune complexes and autoantibodies (anti-double stranded (ds) DNA, antinuclear, and anti-Sm antibodies), and the glomerulonephritis [39,40]. MRL/lpr mice is also pathologically close of the human disease in terms of kidney and brain involvement as well as progressive lymphadenopathy, dermatitis and vasculitis [41,42].

In the present study, we found that $CD11b^+Gr1^+$ cells increased in the early stages of the lupus progression. TLR7 and IFN-α synergistically promoted $CD11b^+Gr1^+$ cells accumulation over myeloid cell differentiation. Furthermore, we identified that mTOR pathway was critical for the accumulation and function of $CD11b^+Gr1^+$ cells in lupus. These findings provide the first clear evidence that mTOR inhibitor INK128 had a good therapeutic action on lupus development via regulating inflammation-induced $CD11b^+Gr1^+$ cells.

2. Results

2.1. The percentage of $CD11b^+Gr1^+$ cells is increased in the early stage of lupus progression

We first detected the expansion of $CD11b^+Gr1^+$ cells in a pristane-induced lupus mouse model. As shown in Fig. 1, the percentage of $CD11b^+Gr1^+$ cells was elevated in bone marrow (BM) (Fig. 1A), peripheral blood mononuclear cell (PBMC) (Fig. 1B) and spleen (Fig. 1C) in the model (7 months), compared to control mice. These data is consistent with our previous findings in MRL/lpr lupus mice and SLE patients [13]. Next, we found that both IFN-α and interferon-stimulated genes (ISGs) expressions were increased in peritoneal exudate cells (PECs) (Fig. 1D), spleen (Fig. 1E) and kidney (Fig. 1F) in pristane-induced lupus mice. To explore when the percentage of $CD11b^+Gr1^+$ cells changed in the lupus progression, the time-course changes of $CD11b^+Gr1^+$ cells were detected. We found that the percentage of $CD11b^+Gr1^+$ cells in spleens was increased after pristane injection for 2 weeks, while the abnormal changes of Th17, Treg, T and B cells did not appear until 28 weeks (Fig. 1G). In MRL/lpr lupus mice, we also found $CD11b^+Gr1^+$ cells increased in the early stages of disease (Supplementary Fig. 1A). These results indicate that the abnormal accumulation of $CD11b^+Gr1^+$ cells may occur in the start-up phase of lupus.

2.2. IFN-α and TLR7 promote $CD11b^+Gr1^+$ cell differentiation in an mTOR-dependent manner in vitro and lupus mice

To explore whether the increased IFN-α contributed to $CD11b^+Gr1^+$ cell accumulation, IFN-α expression was detected in peritoneal exudate cells (PECs), spleen and kidney of pristane-induced lupus mice. The results showed that IFN-α expression correlated positively with $CD11b^+Gr1^+$ cell accumulation (Fig. 2A–C). The expression level of TLR7 was also higher in $CD11b^+Gr1^+$ cells isolated from the lupus mice than that from control mice (Fig. 2F). To investigate the relationship between TLR7 and IFN-α in $CD11b^+Gr1^+$ cells, $CD11b^+Gr1^+$ cells were generated from BM cells cultured in medium supplemented with 40 ng/ml murine IL-6 and 40 ng/ml GM-CSF for 4 days (Fig. 2D) and stimulated BM-derived $CD11b^+Gr1^+$ cells with IFN-α. The results showed that TLR7 expression was significantly upregulated upon IFN-α stimulation (Fig. 2E). Moreover, western blot results showed that the mTOR downstream molecules p-S6 and p-4EBP1 were abnormally activated in $CD11b^+Gr1^+$ cells derived from pristane-induced lupus mice compared with those derived from control mice (Fig. 2G). TLR7 agonist R848 significantly activated an mTOR signal in $CD11b^+Gr1^+$ cells and IFN-α amplified the activation (Fig. 2H). To identify whether the mTOR pathway was involved in TLR7/IFN-α-induced $CD11b^+Gr1^+$ cells accumulation, BM-derived $CD11b^+Gr1^+$ cells were stimulated with R848 and IFN-α in the absence or presence of INK128. The results showed that R848 induced total $CD11b^+Gr1^+$ cell accumulation (Supplementary Fig. 2). Although IFN-α did not induce total $CD11b^+Gr1^+$ cell accumulation (Supplementary Fig. 3), IFN-α synergized with TLR7 to promote $CD11b^+Gr1^+$ cell accumulation in vitro, while INK128 could inhibit the synergized effects (Fig. 2I). Furthermore, INK128 exhibited a better effect on suppressing $CD11b^+Gr1^+$ cells accumulation than the traditional mTOR inhibitor Rapamycin (Supplementary Fig. 4B). Meanwhile, INK128 (100 nM) treatment did not lead to apoptosis of $CD11b^+Gr1^+$ cells (Supplementary Fig. 5C).

To confirm the role of the mTOR pathway in $CD11b^+Gr1^+$ cell expansion in the lupus mouse model, BALB/c mice were injected with 0.5 ml pristane. After 5 months, lupus mice were treated with vehicle, 1 mg/ml INK128 and Rapamycin for another 2 months. As shown in Fig. 3A–D, lupus mice treated with INK128 and Rapamycin had a decreased percentage of $CD11b^+Gr1^+$ cells in BM, PBMC and spleen, compared with vehicle-treated mice. Moreover, the results showed that

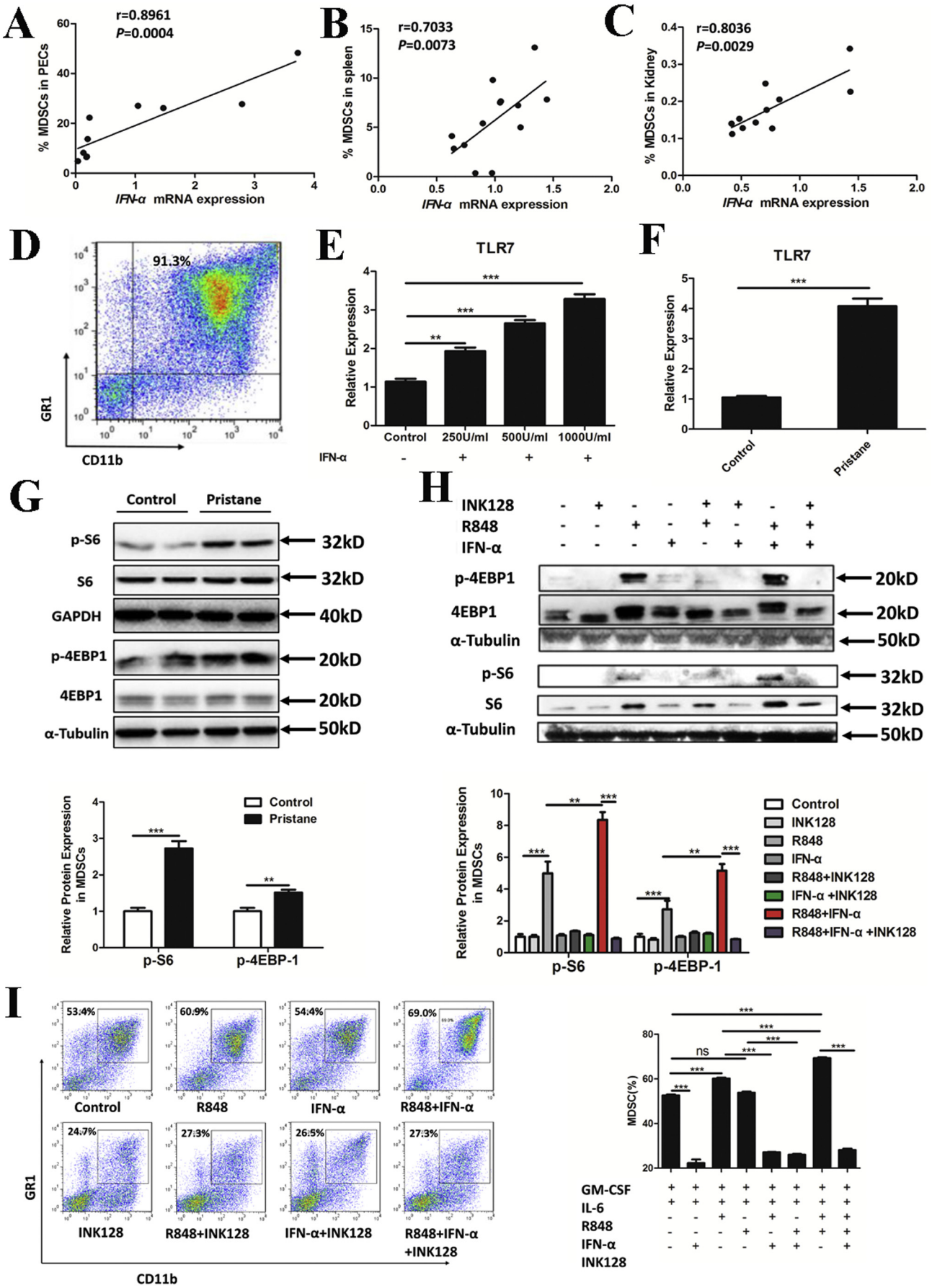

(caption on next page)

Fig. 2. TLR7/IFN-α-mTOR signaling favors $CD11b^+Gr1^+$ cell accumulation during differentiation. Positive correlation between frequency of $CD11b^+Gr1^+$ cells and IFN-α gene expression in PECs (A), spleen (B) and kidney (C) from the control and lupus mice after 28 weeks injection. $CD11b^+Gr1^+$ cells generated from the BM of BALB/c mice (D) were cultured with IFN-α. The mRNA expression of *TLR7* (E) was determined. (F) The TLR7 mRNA expression in $CD11b^+Gr1^+$ cells isolated from spleens of control and lupus mice. (G) Expression of p-4EBP, 4EBP1, p-S6 and S6 in $CD11b^+Gr1^+$ cells isolated from control and lupus mice was detected by western blot (up). The density quantification of band intensities was shown (down). (H) Mouse BM cells were cultured for 4 days in GM-CSF and IL-6 with or without INK128, R848, IFN-α. The expression of p-4EBP, 4EBP1, p-S6 and S6 was detected by western blot (up). The density quantification of band intensities was shown (down). (I) Mouse BM cells were cultured for 4 days in GM-CSF and IL-6 with or without INK128, R848, IFN-α. Percentages of $CD11b^+Gr1^+$ cells were detected. Data were expressed as mean ± SD of three independent experiments. $^*P \le 0.05$, $^{**}P \le 0.01$, $^{***}P \le 0.001$.

INK128 significantly suppressed the IFN-α and ISGs expressions in PECs, spleen and kidney in lupus mice (Fig. 3F–H). TLR7 expression in PECs (Fig. 3H), PBMCs (Fig. 3I) and kidney (Fig. 3J) was also decreased in INK128-treated lupus mice. INK128 has also more effective inhibition on $CD11b^+Gr1^+$ cell accumulation, TLR7 and IFN-α expression when compared with the traditional mTOR inhibitor. In addition, INK128 also inhibited the percentage of $CD11b^+Gr1^+$ cells in MRL/lpr lupus mice (Supplementary Fig. 1B). We also detected the effect of INK128 on the early stage of pristane-induced lupus, BALB/c mice were injected with 0.5 ml pristane followed by INK128 treatment for 2 weeks. INK128 reduced the percentage of $CD11b^+Gr1^+$ cells in PECs and spleens, the early peritoneal and kidney inflammatory response to pristane and IFN-α production (Supplementary Figs. 6, 7). Taken together, these findings demonstrate that IFN-α and TLR7 promote $CD11b^+Gr1^+$ cell differentiation in an mTOR-dependent manner, while mTOR inhibitor INK128 could inhibit $CD11b^+Gr1^+$ cell accumulation in lupus mice.

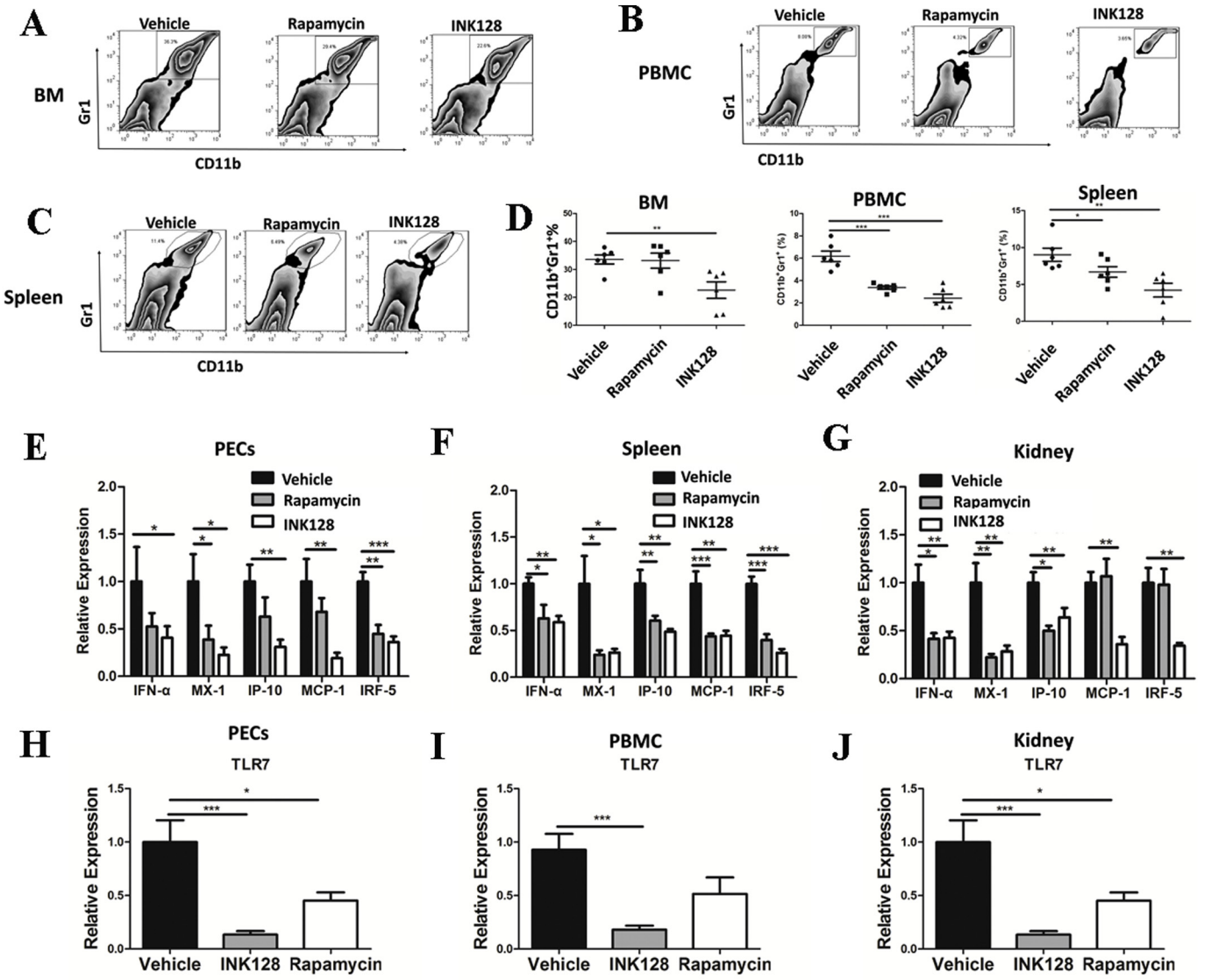

Fig. 3. mTOR inhibitor INK128 can effectively suppress $CD11b^+Gr1^+$ cell abnormal accumulation in lupus mice. BALB/c WT mice (n = 6–8) were given a single injection of 0.5 ml pristane and keep for 5 months. Then mice were INK128 or Rapamycin treated for another 2 months. (A–D) Representative flow cytometry analyses of $CD11b^+Gr1^+$ cells in BM, PBMC and spleen. (E–G) Relative quantitation of *IFN-α* and *ISGs* by RT-PCR in PECs, spleen and kidney from each groups. (H–J) The *TLR7* mRNA expression in PECs, PBMC and kidney from each group. Data were expressed as mean ± SD of three independent experiments. $^*P \le 0.05$, $^{**}P \le 0.01$, $^{***}P \le 0.001$.

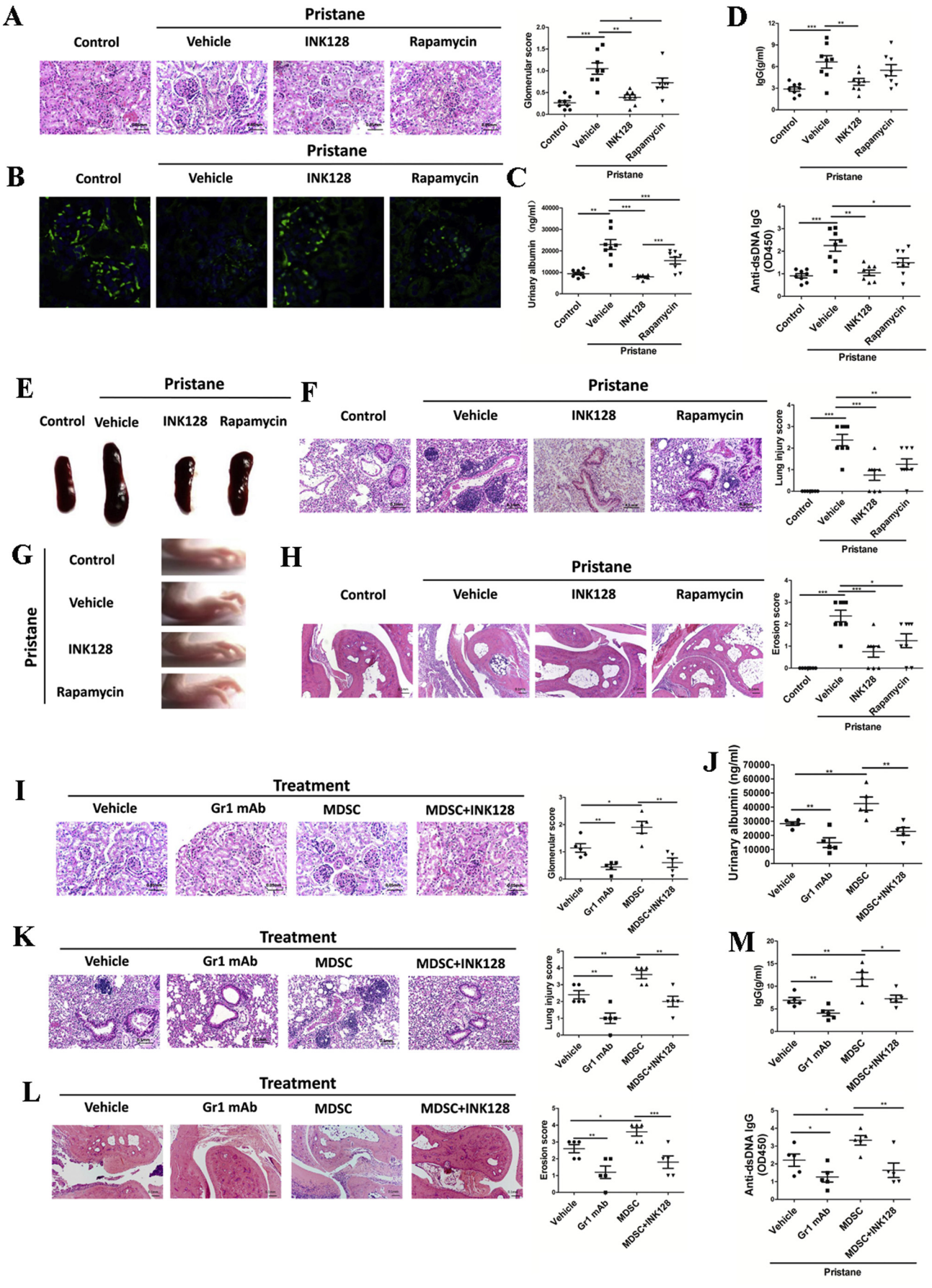

(caption on next page)

Fig. 4. INK128 attenuates disease activity by regulating $CD11b^+Gr1^+$ cells in lupus mice. (A–H) INK128 or Rapamycin-treated lupus mice after 2 months. (A) Kidney sections from each group showed histologic differences. (B) Representative confocal images of kidneys from each groups stained with DAPI (blue) and anti-WT-1 (green) showed podocyte injury. (C) Proteinuria in each group was determined using Mouse Albumin ELISA Quantitation Set. (D) Serum levels of total IgG and IgG against dsDNA were determined by ELISA. (E) Representative photographs of spleens from each group. (F) Lung sections from each groups showed histologic differences. (G) Representative photographs of paws from each group. (H) Representative histological sections of tarsal hind paw joints. (I–M) Gr1 mAb, lupus $CD11b^+Gr1^+$ cells or INK128 treated lupus $CD11b^+Gr1^+$ cells treated mice for 2 months. (I) Kidney sections from each group showed histologic differences. (J) Proteinuria in each group was determined using Mouse Albumin. (K) Lung sections from each groups showed histologic differences. (L) Representative histological sections of tarsal hind paw joints. (M) Serum levels of total IgG and IgG against dsDNA were determined by ELISA Quantitation Set. Representative photographs of paws from each group. Data represent the mean scores ± SEM. $^*P \leq 0.05$, $^{**}P \leq 0.01$, $^{***}P \leq 0.001$.

2.3. mTOR inhibitor INK128 attenuates disease activity of lupus mice related to $CD11b^+Gr1^+$ cells

To determine the therapeutic effect of INK128 on SLE, pristane-induced lupus mice were treated with INK128 for 2 months. As shown in Fig. 4, kidneys from INK128-treated lupus mice showed a better effect on glomerulonephritis and infiltration of lymphoid, compared to vehicle-treated lupus mice (Fig. 4A). Moreover, INK128 gradually increased the expression of the podocyte marker WT1, which was significantly decreased in vehicle-treated lupus mice (Fig. 4B). Similarly, INK128 decreased proteinuria (Fig. 4C), serum IgG and anti-dsDNA IgG levels (Fig. 4D), which were significantly increased in vehicle-treated lupus mice. INK128 also gradually remitted splenomegaly (Fig. 4E) and attenuated lung inflammation which was severe in pristane-induced lupus mice (Fig. 4F). In addition, INK128 attenuated swelling and redness of the hind paw joints (Fig. 4G), and inflammatory infiltration and bone erosion of the tarsal joints in lupus mice (Fig. 4H). The therapeutic effect of INK128 on MRL/lpr lupus mice was also confirmed (Supplementary Fig. 1C–G). These results together indicate INK128 has a therapeutic effect on lupus.

To further explore whether the therapeutic effect of INK128 on lupus was related to the changes of $CD11b^+Gr1^+$ cells, $CD11b^+Gr1^+$ cells were deleted or adoptively transferred. The results showed that $CD11b^+Gr1^+$ cell deletion could improve the lupus symptoms, while adoptive transfer of $CD11b^+Gr1^+$ cells derived from lupus mice could accelerate the disease progression. Moreover, when INK128-treated $CD11b^+Gr1^+$ cells were transferred to the lupus mice, lupus symptoms were not aggravated compared to INK128-untreated $CD11b^+Gr1^+$ cell groups (Fig. 4I–M). Taken together, these results indicated that the therapeutic effect of INK128 on lupus is related to the regulated $CD11b^+Gr1^+$ cells.

2.4. INK128 ameliorates lupus by suppressing TLR7/IFN-α-mTOR signal in $CD11b^+Gr1^+$ cells

To examine whether the function of $CD11b^+Gr1^+$ cells is changed in priatane-induced lupus, we isolated $CD11b^+Gr1^+$ cells from spleens and detected several functional molecules including ROS, NOX components P47 and GP91, Arginase-1 and iNOS. As shown in Supplementary Fig. 8A, ROS production from $CD11b^+Gr1^+$ cells of lupus mice was significantly higher than that from control mice. NOX components P47 and GP91, which are related to ROS production, were also up-regulated in $CD11b^+Gr1^+$ cells from lupus mice (Supplementary Fig. 8B). Moreover, the expressions of Arginase-1 and iNOS in $CD11b^+Gr1^+$ cells from lupus mice were increased compared with those from control mice (Supplementary Fig. 8C–E).

To identify how TLR7 and IFN-α participate in functional changes of $CD11b^+Gr1^+$ cells, BM-derived $CD11b^+Gr1^+$ cells were stimulated with or without R848 and IFN-α for 24 h. The results showed that TLR7 agonist R848 could significantly increase the production of ROS (Fig. 5A), Arginase-1 (Fig. 5B and C) and IL-1β (Fig. 5D) in $CD11b^+Gr1^+$ cells, while IFN-α acted as a cofactor to amplify the action of R848. Interestingly, the regulatory role of TLR7 and IFN-α on MDSCs was indeed synergistic in an mTOR signaling-dependent pattern. Moreover, the production of functional molecules in M-MDSCs and G-MDSCs influenced by TLR7 and IFN-α respectively were shown in Supplementary Fig. 9.

Our previous study showed that G-MDSCs from the diseased MRL/lpr mice impaired Treg differentiation depending on ROS production, while M-MDSCs were highly efficient in promoting the Th17 differentiation via IL-1β [13]. In another study, MDSCs from SLE patients were reported to accelerate the Th17 differentiation in arginase-1-dependent manner [10]. Thus, BM-derived $CD11b^+Gr1^+$ cells were pretreated with or without R848, IFN-α and INK128 and co-cultured with $CD4^+$ T cells. The differentiation of $CD4^+$ T into Tregs or Th17 cells was then detected. The results showed that TLR7-and IFN-α-treated $CD11b^+Gr1^+$ cells could induce more Th17 cells and IL-17A production, but induced less Tregs (Fig. 5E–F). INK128-treated $CD11b^+Gr1^+$ cells could reverse the differentiation of $CD4^+$ T into Tregs or Th17 cells induced by TLR7-and IFN-α-treated $CD11b^+Gr1^+$ cells (Fig. 5E–F).

We also determined the regulation of INK128 on $CD11b^+Gr1^+$ cells for maintaining Th17/Treg balance in spleens and kidneys of lupus mice. The results showed that INK128 indeed down-regulated the frequency of Th17 cells and up-regulated the frequency of Tregs in kidney and spleens (Fig. 5G–J). Furthermore, $CD11b^+Gr1^+$ cell deletion could maintain Th17/Tregs balance, while adoptive transferring of $CD11b^+Gr1^+$ cells derived from lupus mice could accelerate the unbalance of Th17/Tregs. When transfer INK128-treated $CD11b^+Gr1^+$ cells to the lupus mice, the unbalance of Th17/Tregs was not aggravated compared to INK128-untreated $CD11b^+Gr1^+$ cells groups (Fig. 5K–L). In addition, INK128 also improved the unbalance of Th17/Tregs in MRL/lpr mice (Supplementary Fig. 1E and F). Moreover, compared to Rapamycin, INK128 more effectively regulated the unbalance of Th17/Tregs in lupus. Taken together, these findings demonstrate that INK128 ameliorates lupus via suppression of TLR7/IFN-α-mTOR signal in $CD11b^+Gr1^+$ cells for improvement of Th17/Treg balance.

2.5. INK128 reduces TLR7/IFN-α-induced $CD11b^+Gr1^+$ cells differentiation into macrophages in lupus nephritis

In chronic inflammation, MDSCs have potential to differentiate to macrophages [43]. Lupus nephritis is an inflammation of the kidneys caused by SLE and often results in progressive renal dysfunction. Of note, the infiltrating macrophages contribute to ongoing renal injury. It is unclear whether TLR7/IFN-α-modified $CD11b^+Gr1^+$ cells promote macrophage development in lupus nephritis. Our results showed that INK128 reduced significantly $CD11b^+F4/80^+$ macrophages in kidneys (Fig. 6A) and the production of inflammatory factors (Fig. 6B) in pristane-induced lupus mice. INK128 also inhibited more effectively macrophage differentiation in lupus compared to Rapamycin. In addition, INK128 also inhibited the macrophage accumulation in kidneys in MRL/lpr mice (Supplementary Fig. 1G).

To explore, whether mTOR signal was involved in differentiation of $CD11b^+Gr1^+$ cells into macrophages during the pathogenesis of lupus nephritis, BM-derived $CD11b^+Gr1^+$ cells were incubated with GM-CSF for 3 days and 5 days following treatment with or without R848, IFN-α and INK128. On day 3 and day 5, R848-treated $CD11b^+Gr1^+$ cells displayed a significantly greater differentiation capacity into $F4/80^+$ cells and IFN-α as a cofactor could enhance the action of R848. In contrast, INK128 suppressed the differentiation capacity of

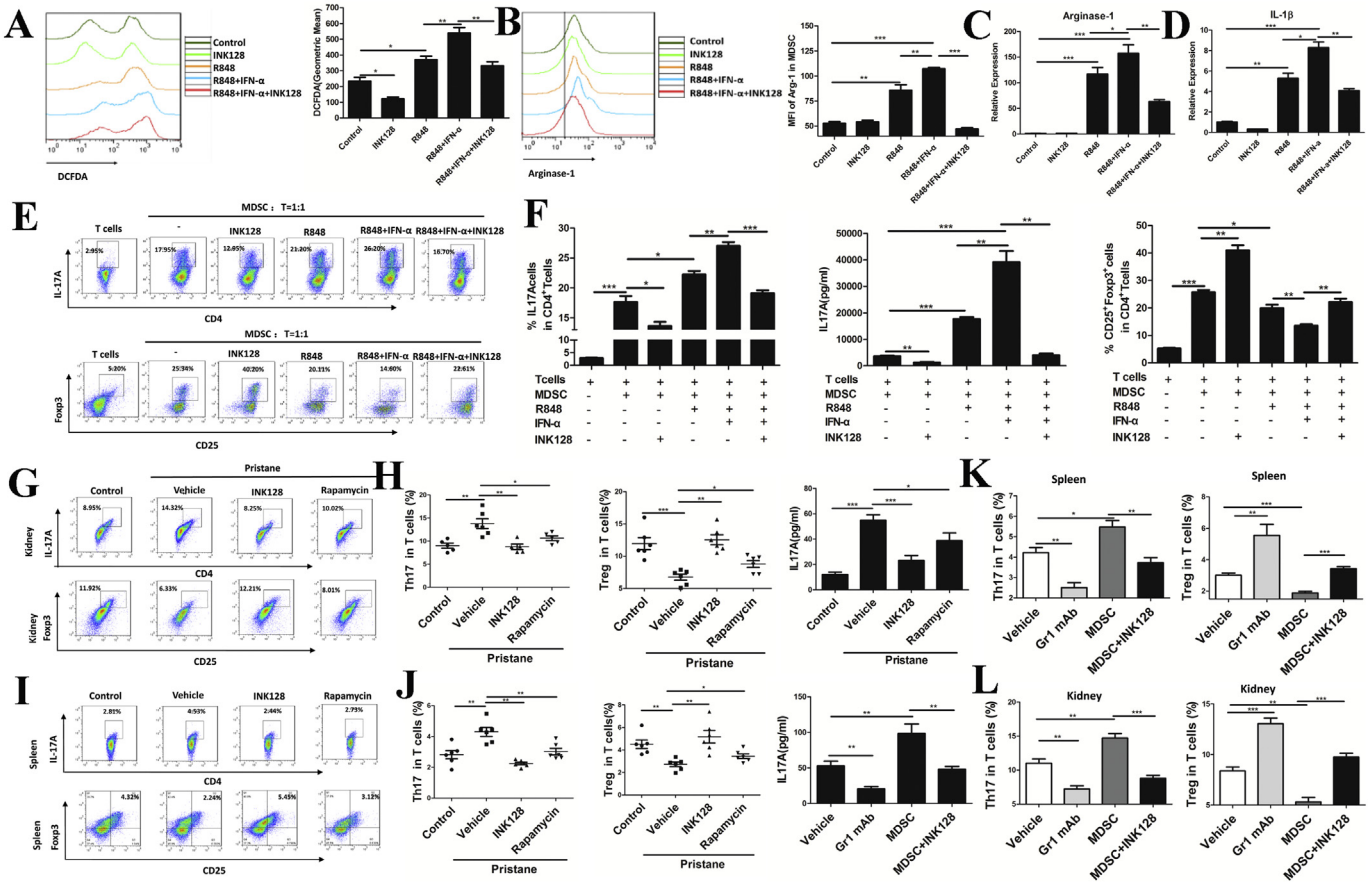

Fig. 5. INK128 ameliorates unbalance of Th17/Treg in lupus mice by regulating TLR7/IFN-α-mTOR signal in CD11b$^+$Gr1$^+$ cells. BM-derived CD11b$^+$Gr1$^+$ cells were treated with or without INK128, R848, IFN-α for 24 h. Fluorescence intensity of DCFDA (A) and Arginase-1 (B) was measured by flow cytometry. (C) The *Arginase-1* mRNA expression level in each group was assayed. (D) The *iNOS* mRNA expression level in each group was assayed and NO concentration was detected. (E) The *IL-1β* mRNA expression level in each group was assayed by RT-PCR. Splenic T cells from wide-type BALB/c mice were cultured in the presence of CD11b$^+$Gr1$^+$ cells pretreated with or without INK128, R848 and IFN-α for 24 h and differentiated into Th17 or Treg cells for another 3 days. (E) The percentages of Th17 cells and Treg cells were assayed by flow cytometry. (F) The statistical analyses of the percentage of Th17 cells (left) and Treg cells (right) are shown. Supernatant IL-17A levels were measured in the Th17-polarizing culture system by ELISA assays (middle). (G–J) BALB/c WT mice (n = 6–8) were given a single injection of 0.5 ml pristane and keep for 5 months. Then INK128-or Rapamycin-treated mice for another 2 months. (G) The percentages of Th17 cells and Treg cells in kidney from each group were assayed by flow cytometry. (H) The statistical analyses of the percentage of Th17 cells (left) and Treg cells (middle) are shown. Supernatant IL-17A levels were measured in the Th17-polarizing culture system by ELISA assays (right). (I) The percentages of CD4$^+$IL17A$^+$ Th17 cells and CD4$^+$CD25$^+$ Foxp3$^+$ Treg cells in spleens from each groups were assayed by flow cytometry. (J) The statistical analyses of the percentage of Th17 cells (left) and Treg cells (middle) are shown. Supernatant IL-17A levels were measured in the Th17-polarizing culture system by ELISA assays (right). (K–L) BALB/c WT mice (n = 5) were given a single injection of 0.5 ml pristane and keep for 5 months. Then Gr1 mAb, lupus CD11b$^+$Gr1$^+$ cells or INK128-treated lupus CD11b$^+$Gr1$^+$ cells in treated mice for another 2 months. The percentages of Th17 cells and Treg cells in spleens (K) and kidney (L) from each group were assayed by flow cytometry. Representative results of three independent experiments are shown. Data represent the mean scores ± SEM. $^*P \le 0.05$, $^{**}P \le 0.01$, $^{***}P \le 0.001$.

CD11b$^+$Gr1$^+$ cells (Fig. 6C–D). Furthermore, we identified that CD11b$^+$Ly6C$^+$Ly6G$^-$ cells rather than CD11b$^+$Ly6C^{low}Ly6G$^+$ cells mainly contributed to the differentiation into macrophages (Fig. 6E–F). Some studies have suggested that the S100A8 and S100A9 proteins are directly involved in inhibiting CD11b$^+$Gr1$^+$ cell maturation [43]. Our results showed that TLR7 and IFN-α signaling synergistically decreased the levels of both S100A8 and S100A9 mRNAs at day 3 and day 5 depending on the mTOR pathway (Fig. 6G–H). TLR7 signaling significantly increased F4/80 (Fig. 6I) and MHC-II (Fig. 6J) expressions in R848-treated CD11b$^+$Gr1$^+$ cells. In addition, BM-derived CD11b$^+$Gr1$^+$ cells incubated with GM-CSF for 5 days following treatment with R848 and IFN-α. The results showed that TLR7 and IFN-α signaling synergistically promoted production of inflammatory factors (IL-1β, IL-6 and IL12p40) and chemokines (MCP-1) (Fig. 6K). Taken together, these findings demonstrate that INK128 also ameliorates lupus nephritis via suppressing the differentiation of CD11b$^+$Gr1$^+$ cells into macrophages in lupus.

3. Discussion

Recently, functions of MDSCs in development and regulation of SLE have started to get attention. However, MDSCs showed a variety of activities and effects in SLE models and diseases. MDSCs functions in SLE are controversial. Our previous studies have identified that CD11b$^+$Gr1$^+$ cells is increased both in female patients with SLE and in two kinds of lupus mice models. We also found that CD11b$^+$Gr1$^+$ cell functions have changed in SLE conditions [13]. Our recent works revealed that activated TLR7 signal influenced CD11b$^+$Gr1$^+$ cell expansion and functions, demonstrated that IFN-α was an essential cofactor in these progress, and identified the TLR7-mTOR pathway as critical for CD11b$^+$Gr1$^+$ cell accumulation and functions which were contribute to lupus development. We also firstly evaluated that the second generation mTOR inhibitor INK128 had a good therapeutic action in lupus development by regulating CD11b$^+$Gr1$^+$ cells.

In this research, we explore the time course changes of CD11b$^+$Gr1$^+$ cells in two lupus mice model and found that the

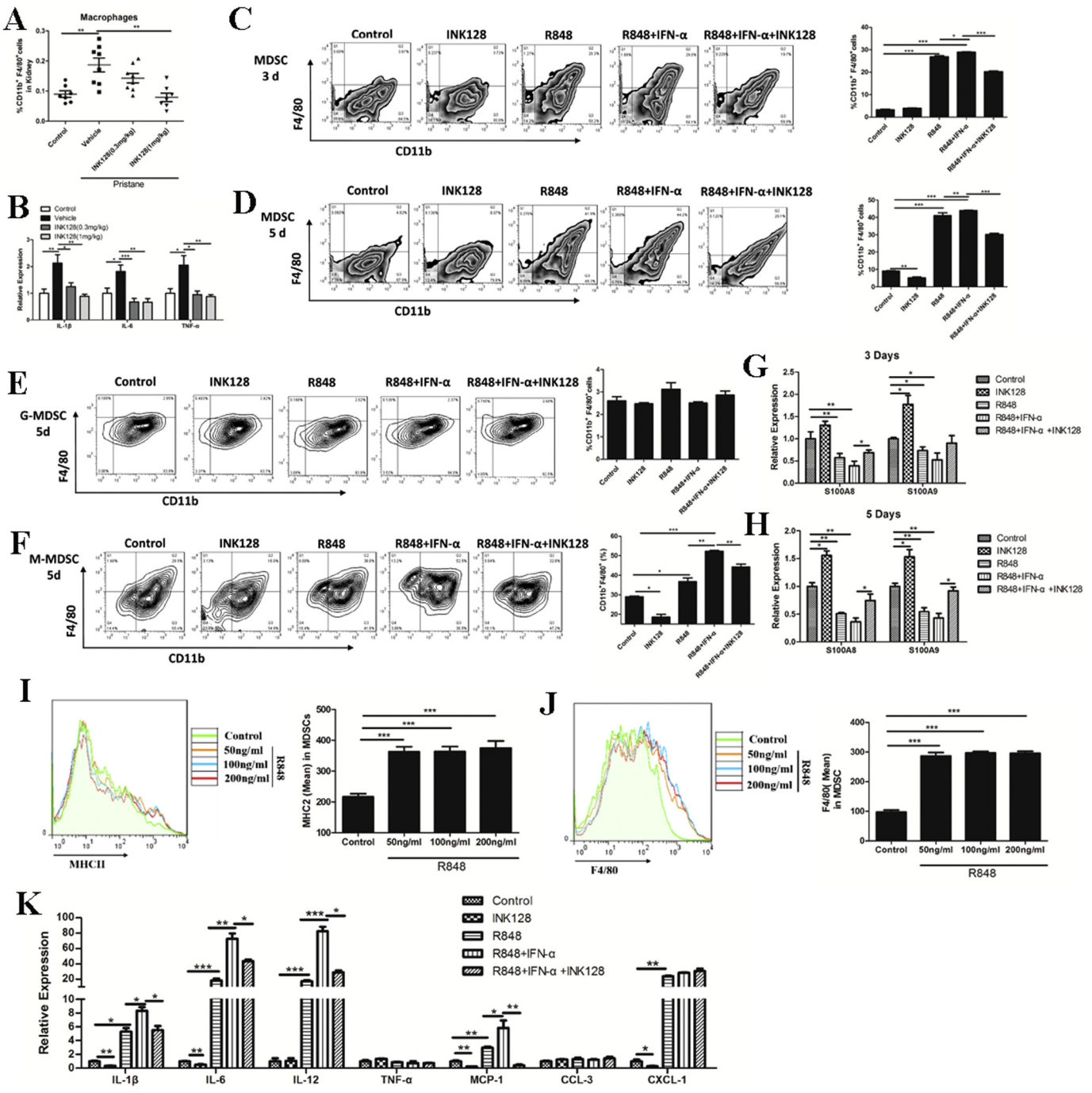

Fig. 6. INK128 decreases macrophage accumulation in lupus nephritis by regulating TLR7/IFN-α-mTOR signal in $CD11b^+Gr1^+$ cells. BALB/c WT mice (n = 6–8) were given a single injection of 0.5 ml pristane and kept for 5 months. Then mice were INK128 or Rapamycin-treated for another 2 months. (A) The percentages of macrophages in kidney cells were assayed. (B) The mRNA expression of cytokines IL-1β, IL-6 and TNF-α in each group. (C–D) BM-derived $CD11b^+Gr1^+$ cells were treated with or without INK128, R848 and IFN-α for 3 days and 5 days. The percentages of macrophages were assayed. (E–F) G-MDSCs and M-MDSCs isolated from BM-derived $CD11b^+Gr1^+$ cells were treated with or without INK128, R848 and IFN-α for 5 days. The percentages of macrophages differentiated from G-MDSCs and M-MDSCs were assayed. (G–H) *S100A8* and *S100A9* mRNA expression in $CD11b^+Gr1^+$ cells was assayed. (I–J) BM-derived $CD11b^+Gr1^+$ cells were treated with or without INK128, R848 and IFN-α for 5 days. Makers of immature phenotype, such as MHCII (I) and F4/80 (J) from $CD11b^+Gr1^+$ cells were examined. (K) BM-derived $CD11b^+Gr1^+$ cells were treated with or without INK128, R848 and IFN-α for 5 days. The mRNA expression of cytokines and chemokines in $CD11b^+Gr1^+$ cells was determined. Representative results of three independent experiments are shown. Data represent the mean scores ± SEM. $^*P \le 0.05$, $^{**}P \le 0.01$, $^{***}P \le 0.001$.

percentage of $CD11b^+Gr1^+$ cells increased prior to the abnormal changes of Th17, Treg, T and B cells in lupus development. These results indicated that the abnormal accumulation of $CD11b^+Gr1^+$ cells may play a crucial role in the start-up phase of lupus. Furthermore, we found $CD11b^+Gr1^+$ cells were increased in multiple organs of the pristane-induced lupus mice, which correlated positively with IFN-α expression and ISGs. In addition, high IFN-α levels in kidneys from pristane-induced lupus mice were correlated positively with TLR7 expression levels. The nucleic acid–sensing intracellular TLR7 is expressed at the highest levels in B cells and pDCs, which may help to explain why these cells play an important part in the pathogenesis of SLE. Mice that overexpressing TLR7 can develop a lupus-like disease, and lupus mice

that are rendered deficient in TLR7 are protected from lupus [44]. In this study, we found TLR7 expression in $CD11b^+Gr1^+$ cells was increased in pristane-induced lupus mice compared with WT BALB/c mice. We also proved that TLR7 expression in $CD11b^+Gr1^+$ cells is dependent on IFN-α. Previous studies have reported that type I IFN can maintain TLR7 expression levels in B cells and dendritic cells to regulate TLR7-dependent inflammation [45–47].

In a lupus microenvironment, nucleic acids antigens released from the dead and dying cells can activate a TLR7 signal in the early disease. A Recent study showed that TLR7 signal induced myeloid expansion in the mice with transgenic overexpression of TLR7 and type I IFN participated in this process [32]. We found that TLR7 agonist R848 administration specifically increased $CD11b^+Gr1^+$ cell generation during differentiation in vitro. Although IFN-α did not influenced the total proportion of $CD11b^+Gr1^+$ cells, $CD11b^+Ly6C^+Ly6G^-$ cells showed a concentration-dependent increase and $CD11b^+Ly6C^{low}Ly6G^+$ showed a concentration-dependent decrease in the presence of IFN-α.

We detected the molecular mechanisms by which these pathways act to promote $CD11b^+Gr1^+$ cell differentiation from the bone marrow progenitors. Our work demonstrated that IFN-α is an essential cofactor in TLR7-induced $CD11b^+Gr1^+$ cells accumulation from bone marrow progenitors, and identified the TLR7-mTOR pathway as critical for $CD11b^+Gr1^+$ cell expansion. Correspondingly, when injecting the mTOR inhibitor INK128 to lupus mice, we found that $CD11b^+Gr1^+$ cells were decreased significantly in multiple organs, while IFN-α and ISGs levels were also decreased. In humans, two pathways have been implicated in the activation of TLR7 [48]. The first pathway is the LL37 pathway [49] and some molecules such as HMGB1, which can transfer nucleic acids into the cell. The second pathway is the entry of immunoglobulin (IgG) antibodies binding DNA or RNA through FcgR2A into PDCs, leading to TLR7-induced type-I IFN [19,50–52]. In pristane induced lupus mice, the production of IFN-α was primarily secreted by M-MDSCs in early disease. Therefore, inhibiting $CD11b^+Gr1^+$ cells in the early stage of lupus may be a therapeutic plan to slow down lupus progression. Our studies showed that an activated mTOR signal in $CD11b^+Gr1^+$ cells played significant roles in accumulation. We evaluated a bioavailable, highly potent and selective mTOR inhibitor INK128 in pristane-induced lupus mice for the first time. INK128 can decrease $CD11b^+Gr1^+$ cell accumulation in kidney, attenuate LN by decreasing the numbers of the inflammatory cells, reduced the glomerular injury in kidney and reduced the inflammatory cell infiltration in joints and lungs.

Tregs were decreased and Th17 cells were increased in our pristane-induced lupus mice. In our previous study, G-MDSCs from diseased MRL/lpr mice impair Treg differentiation depending on ROS production and M-MDSCs were highly efficient in promoting the Th17 differentiation via IL-1β [13] In another study, MDSCs from SLE patients accelerated the Th17 differentiation in an arginase-1-dependent manner [10]. In this study, molecules regulating the Th17/Tregs balance in $CD11b^+Gr1^+$ cells were changed greatly following by TLR7 and IFN-α stimulation. Therefore, $CD11b^+Gr1^+$ cells modified by TLR7 and IFN-α could promote the abnormal Th17/Tregs balance significantly via the mTOR pathway. Lupus nephritis (LN), is seen in up to 60% of SLE patients [53]. Macrophages are believed to contribute to the pathogenesis of LN [53–55]. Some studies reported that $CD11b^+Gr1^+$ cells have the potential of differentiation to macrophages in chronic inflammation [43]. Did TLR7-and IFN-α-modified $CD11b^+Gr1^+$ cells promote macrophage development in the lupus progress? In this study, we found that $CD11b^+Gr1^+$ cells and macrophages are both increased in pristane-induced lupus mice, and $CD11b^+Gr1^+$ cells treated with R848/IFN-α could differentiate into macrophages. In addition, $CD11b^+Gr1^+$ cells treated with R848 showed a mature inflammatory phenotype and produced more inflammatory factors, which contributed to LN. The mTOR signal activated by TLR7 and IFN-α stimulation played an important role in promoting $CD11b^+Gr1^+$ cell differentiation to macrophages through maintaining S100A8 and S100A9 expression.

In infectious disease and cancer MDSCs play deleterious roles in the disease progress, but the role of MDSCs in autoimmune disease is more complex [56]. Although these contrasting studies show positive and negative roles for MDSCs in the regulation of SLE development, these different roles for MDSCs are apparently due to the different severities of SLE and specifics of the microenvironment. Intravenous treatment with MDSCs obtained from normal C57BL/6 mice ameliorated autoimmunity in $Roquin^{san/san}$ lupus mice [8]. However, G-MDSC from the (NZB × NZW) F1 lupus mice with established disease showed functional defects [11]. MDSCs from SLE patients promoted Th17 differentiation in an Arginase-1-dependent manner and accelerated the progress of SLE [10]. These studies suggested that the factors in lupus microenvironment may result in MDSCs functional differences comparing to the MDSCs in non-disease conditions. In a lupus microenvironment, activated TLR7 signal by endogenous nucleic acids released from apoptotic or necrotic cells and elevated level of IFN-α is a driving pathogenic force for most SLE patients based on substantial genetic, epidemiologic and clinical data [15–20]. Our work showed that TLR7 signals and IFN-α signals played very important roles in $CD11b^+Gr1^+$ cells expansion and functions in lupus microenvironment. Therefore, studying $CD11b^+Gr1^+$ cell differences in disease and health condition will be of great significance to explore the specific role of $CD11b^+Gr1^+$ cells in SLE progression.

In conclusion, results presented here provide an insight into the relationship between some factors (TLR7 ligand and IFN-α) from the lupus cellular microenvironment and $CD11b^+Gr1^+$ cell accumulation and functions during SLE. BM-derived $CD11b^+Gr1^+$ cells were stimulated with R848 and IFN-α in the absence or presence of mTOR inhibitor INK128. We found that R848 accelerated GM-CSF-and IL-6-induced total $CD11b^+Gr1^+$ cell accumulation and IFN-α synergized with TLR7 to promote this progress, while mTOR inhibitor INK128 could inhibit the synergized effects. Our work defined at a molecular level how the TLR7 signal influenced $CD11b^+Gr1^+$ cell expansion and functions, demonstrated that IFN-α is an essential cofactor in this process, and identified the TLR7/ IFN-α-mTOR pathway as critical for GM-CSF-and IL-6-induced $CD11b^+Gr1^+$ cell accumulation and functions, which contributed to lupus development. We also provide evidence for the first time that INK128, a second generation mTOR inhibitor, has a good therapeutic action in lupus development by regulating $CD11b^+Gr1^+$ cells.

4. Methods

4.1. Antibodies and reagents

Antibodies with the following specificities were used for all analyses: CD11b (M1/70), Gr1 (RB6-8C5), F4/80 (BM8), CD4 (GK1.5), Foxp3 (MF-14), CD25 (3C7), IL-17A (TC11-18H10.1) and MHCII (M5/114.15.2) (all from Biolegend). Arginase-1/ARG-1 (IC5868P) and mTOR (303728) (all from R&D Systems). Anti-CD3 mAb (145-2C11), anti-CD28 mAb (37.51), anti-IL-4 mAb (11B11) and anti-IFN-γ mAb (XMG1.2) (all from Biolegend). Antibodies for α-Tubulin (2144), p-S6 (4858S), S6 (2217S), p-4EBP-1 (2855S) and 4EBP-1 (9644T) (all from cell Signal Technology Inc). MLN0128 / INK128 and Rapamycin (Selleckchem). Recombinant mouse IFN-α2 (eBiocience). Recombinant mouse IL-6, GM-CSF, $CD4^+$ T Cell Isolation Kit and MDSC Isolation Kit (all from Miltenyi Biotec). Recombinant mouse/human TGF-β (Peprotech). The oxidation-sensitive dye DCFDA and NO detection Kit (all from Beyotime). LPS and R848 (Enzo Life Science). Trizol Reagent and SYBR green dye (Invitrogen). The Dulbecco's modified Eagle medium (DMEM) and fetal bovine serum (FBS) (Gibco). Collagenase type D and DNase I (Roche. Sterile) pristane, *N*-methyl-2-pyrrolidone (NMP) and polyvinyl pyrrolidone (PVP), PMA, ionomycin and brefeldin A (BFA) (all from Sigma). Mouse Albumin ELISA Quantitation Set (Bethyl Laboratories). Mouse IL17A ELISA Quantitation Set

(Peprotech). Mouse anti-IgG and anti-dsDNA IgG Kit (Bethyl Laboratories, Montgomery, USA).

4.2. Mice

Female BALB/c mice (6–8 weeks old) and female MRL/lpr mice were from Model Animal Research Center of Nanjing University (Nanjing, PR China) and were housed in pathogen-free conditions in a 12-h light and dark cycle. All procedures involving mice were approved by the institutional license for animal care and use based on the Animal Care Committee at Nanjing University. The method to induce lupus mice model by pristane and the INK128 or Rapamycin treatment are presented in Supplementary Methods 1.

4.3. Isolation of $CD11b^+Gr1^+$ cells

Bone marrow (BM) cells were isolated as described previously [13,57]. In brief, tibias and femurs were removed from BALB/c mice and BM cells were flushed. Then BM cells were cultured in the medium supplemented with 40 ng/ml murine IL-6 and 40 ng/ml GM-CSF in the absence or presence of R848, IFN-α and INK128 for 4 days. BM-derived $CD11b^+Gr1^+$ cells and Spleen-derived $CD11b^+Gr1^+$ cells were purified from pristane-induced lupus mice using Myeloid-Derived Suppressor Cell Isolation Kit. G-MDSCs and M-MDSCs were purified from BM-derived MDSCs mice using Myeloid-Derived Suppressor Cell Isolation Kit.

4.4. Generation of BM-derived $CD11b^+Gr1^+$ cells

BM cells were isolated from mice by flushing femurs and tibiae. Then BM cells were centrifuged and re-suspended in culture medium supplemented with murine IL-6 (40 ng/ml; Miltenyi Biotec, Auburn, CA) and GM-CSF (40 ng/ml; Miltenyi Biotec, Auburn, CA), and these cells were cultured for 4 days. To get higher purity $CD11b^+Gr1^+$ cells, we only separate the suspension cells in the dishes.

4.5. $CD11b^+Gr1^+$ cells depletion

20 week old pristane-induced lupus mice were injected i.p. with anti-Gr-1 antibodies (RB6-8C5, 200 μg; Biolegend, San Diego, USA) once every 4 d.

4.6. Treatment

For $CD11b^+Gr1^+$ cell depletion in vivo, 20 week old pristane-induced lupus mice were injected i.p. with anti-Gr-1 antibodies once every 4 d. When used for adoptive transfer, 2×10^6 $CD11b^+Gr1^+$ cells isolated from the lupus mice were washed twice and resuspended in 200 μl PBS and injected in mice via the tail vein.

4.7. ROS detection

Reactive oxygen species (ROS) production was measured by the oxidation-sensitive dye DCFDA. $CD11b^+Gr1^+$ cells were incubated at 37 °C in Roswell Park Memorial Institute (RPMI) medium in the presence of 2.5 μM DCFDA and simultaneously cultured with 1 μg/ml LPS for 30 min. Then cells were washed with PBS and measured by the flow cytometry (Becton Dickinson, San Diego, USA).

4.8. Th17 cell and $CD4^+CD25^+Foxp3^+$ Treg differentiation

$CD4^+$ T cells were purified from BALB/c mice by using $CD4^+$ T Cell Isolation Kit. MDSCs are pretreated with or without INK128, IFN-α and R848 for 24 h. $CD4^+$ Cells were stimulated by anti-CD3 (5 μg/ml) and anti-CD28 (5 μg/ml) in the culture with 2.5 ng/ml hTGF-β, 20 ng/ml IL-6, 10 μg/ml of anti-IL-4 mAb and anti-IFN-γ mAb in 24-well plates. In the meantime, pretreated $CD11b^+Gr1^+$ cells were added to the culture on day 0 at a ratio of 1:1and cells were cultured in triplicate in culture medium. On day 3, cells were stimulated with 5 ng/ml phorbol myristate acetate (PMA), 1 ng/ml ionomycin for and10 ng/ml brefeldin A for 5 h. Then cells were stained with FITC-conjugated anti-mouse CD4 mAb. After cells permeabilization with Cytofix/Cytoperm, cells were stained with APC-conjugated anti-mouse IL17A mAb, then cells were stained for 30 min at 4 °C in the dark. After washing with buffer, cells were analyzed by flow cytometry. After three days activation, supernatants were collected for IL-17A cytokine assays by ELISA according to the manufacturer's instructions. $CD4^+$T cells were cultured with anti-CD3 (5 μg/ml) and anti-CD28 (5 μg/ml) mAbs in the presence of 5 ng/ml TGF-β in a 24-well plate for 72 h in complete RPMI medium (5×10^5 cells/well). In the meantime, pretreated $CD11b^+Gr1^+$ cells were added to the culture on day 0 at a ratio of 1:1.After 72 h, cells were permeated with Cytofix/Cytoperm, then stained with PE-conjugated anti-mouse Foxp3 mAb. After washing, cells were stained with FITC-conjugated anti-mouse CD4 mAb and APC-conjugated anti-mouse CD25 mAb, then cells were stained for 30 min at 4 °C in the dark. After washing with buffer, cells were analyzed by flow cytometry.

4.9. $CD11b^+Gr1^+$ cell differentiation assay

BM-derived $CD11b^+Gr1^+$ cells were cultured in the presence of 10 ng/ml GM-CSF for 3 and 5 days. In some experiments, 100 ng/ml of R848, 500 U IFN-α and 50 nM INK128 were incubated with GM-CSF. After the different incubation periods, cell phenotypes were determined by flow cytometry analysis.

4.10. Flow cytometry analysis

Cells were immunostained with various combinations of the fluorescence-conjugated antibodies, the detailed methods are represented in Supplementary Material and Method 2.

4.11. RNA extraction and quantitative real-time PCR

Total RNA was isolated using Trizol Reagent according to the manufacturer's instructions. Real-time PCR assay was performed using SYBR green dye on Step One sequence detection system (Applied Biosystems, Waltham, MA, USA). Relative abundance of genes was calculated using $2^{-\Delta\Delta CT}$ formula, and GAPDH as internal control. Primers can be found in the Supplementary table.

4.12. Western blot analysis

Proteins were extracted by standard techniques [58]. Antibodies for p-S6, S6, p-4EBP-1, 4EBP-1, horseradish peroxides (HRP)-conjugated anti-rabbit IgG for western blot were from Cell Signaling Technology (Danvers, MA, USA). Protein bands were visualized using ECL Plus Western blotting detection reagents (Millipore, Bedford, MA, USA). In our studies, α-Tubulin was used as an internal control.

4.13. Cytokines ELISA

Anti-IgG and anti-dsDNA IgG were analyzed using mouse anti-IgG and anti-dsDNA IgG Kit and the sera were applied at dilutions of 1:100,000 and 1:300,000 according to the manufacturer's instructions. Total urinary protein was determined using a Mouse Albumin ELISA Quantitation Set and the urine was applied at dilutions of 1:100 according to the manufacturer's instructions. According to the manufacturer's instructions, cytokine analysis was performed using mouse IL-17A ELISA Kit. Absorbance was determined using ELx-800 Universal Microplate Reader (BIO-TEK, Vermont USA).

4.14. Histologic and immunohistochemical analyses

Sections were cut from paraffin-embedded tissue, fixed in formalin and stained with hematoxylin and eosin.

4.15. Statistics

Results were expressed as mean ± SEM of three independent experiments and each experiment included triplicate sets. Data were statistically evaluated by one-way ANOVA followed by Dunnett's test between control group and multiple dose groups. $P < 0.05$ was considered of statistically significant difference.

Declarations of interest

The authors declare no commercial or financial conflicts of interest.

Author contributions

SGP designed experiments. SGP and LD performed experiments; DH, RJ, LXJ analyzed date. XJJ and DL supervised the research. HYY and SGP wrote the manuscript.

Transparency document

The Transparency document associated with this article can be found, in online version.

Acknowledgement

This work was supported by Natural Science Foundation of China (31872732 and 91542113) and the Fundamental Research Funds for the Central Universities (021414380342).

Appendix A. Supplementary data

Supplementary data to this article can be found online at https://doi.org/10.1016/j.bbadis.2018.10.007.

References

[1] T. Koutsokeras, T. Healy, Systemic lupus erythematosus and lupus nephritis, Nat. Rev. Drug Discov. 13 (2014) 173–174.
[2] G.C. Tsokos, M.S. Lo, P. Costa Reis, K.E. Sullivan, New insights into the immunopathogenesis of systemic lupus erythematosus, Nat. Rev. Rheumatol. 12 (2016) 716–730.
[3] J. Choi, S.T. Kim, J. Craft, The pathogenesis of systemic lupus erythematosus-an update, Curr. Opin. Immunol. 24 (2012) 651–657.
[4] M. Morell, N. Varela, C. Maranon, Myeloid Populations in Systemic Autoimmune Diseases, vol. 53, (2017), pp. 198–218.
[5] J.E. Talmadge, D.I. Gabrilovich, History of myeloid-derived suppressor cells, Nat. Rev. Cancer 13 (2013) 739–752.
[6] D.I. Gabrilovich, S. Nagaraj, Myeloid-derived suppressor cells as regulators of the immune system, Nat. Rev. Immunol. 9 (2009) 162–174.
[7] E.V. Lourenco, M. Wong, B.H. Hahn, M.F. Palma-Diaz, B.J. Skaggs, Laquinimod delays and suppresses nephritis in lupus-prone mice and affects both myeloid and lymphoid immune cells, Arthritis Rheumatol. 66 (2014) 674–685.
[8] M.J. Park, S.H. Lee, E.K. Kim, E.J. Lee, S.H. Park, S.K. Kwok, M.L. Cho, Myeloid-derived suppressor cells induce the expansion of regulatory B cells and ameliorate autoimmunity in the sanroque mouse model of systemic lupus erythematosus, Arthritis Rheumatol. 68 (2016) 2717–2727.
[9] A. Trigunaite, A. Khan, E. Der, A. Song, S. Varikuti, T.N. Jorgensen, Gr-1(high) CD11b+ cells suppress B cell differentiation and lupus-like disease in lupus-prone male mice, Arthritis Rheum. 65 (2013) 2392–2402.
[10] H. Wu, Y. Zhen, Z. Ma, H. Li, J. Yu, Z.G. Xu, X.Y. Wang, H. Yi, Y.G. Yang, Arginase-1-dependent promotion of TH17 differentiation and disease progression by MDSCs in systemic lupus erythematosus, Sci. Transl. Med. 8 (2016) 331ra340.
[11] K. Vlachou, K. Mintzas, M. Glymenaki, M. Ioannou, G. Papadaki, G.K. Bertsias, P. Sidiropoulos, D.T. Boumpas, P. Verginis, Elimination of granulocytic myeloid-derived suppressor cells in lupus-prone mice linked to reactive oxygen species-dependent extracellular trap formation, Arthritis Rheumatol. 68 (2016) 449–461.
[12] G. Dong, M. You, H. Fan, J. Ji, L. Ding, P. Li, Y. Hou, 17beta-estradiol contributes to the accumulation of myeloid-derived suppressor cells in blood by promoting TNF-alpha secretion, Acta Biochim. Biophys. Sin. 47 (2015) 620–629.
[13] J. Ji, J. Xu, S. Zhao, F. Liu, J. Qi, Y. Song, J. Ren, T. Wang, H. Dou, Y. Hou, Myeloid-derived suppressor cells contribute to systemic lupus erythaematosus by regulating differentiation of Th17 cells and Tregs, Clin. Sci. 130 (2016) 1453–1467.
[14] D. Zhang, J. Xu, J. Ren, L. Ding, G. Shi, D. Li, H. Dou, Y. Hou, Myeloid-derived suppressor cells induce podocyte injury through increasing reactive oxygen species in lupus nephritis, Front. Immunol. 9 (2018) 1443.
[15] R.M. Clancy, A.J. Markham, J.P. Buyon, Endosomal Toll-like receptors in clinically overt and silent autoimmunity, Immunol. Rev. 269 (2016) 76–84.
[16] L. Ronnblom, G.V. Alm, A pivotal role for the natural interferon alpha-producing cells (plasmacytoid dendritic cells) in the pathogenesis of lupus, J. Exp. Med. 194 (2001) F59–F63.
[17] L. Ronnblom, M.L. Eloranta, The interferon signature in autoimmune diseases, Curr. Opin. Rheumatol. 25 (2013) 248–253.
[18] J. Di Domizio, W. Cao, Fueling autoimmunity: type I interferon in autoimmune diseases, Expert. Rev. Clin. Immunol. 9 (2013) 201–210.
[19] K.B. Elkon, A. Wiedeman, Type I IFN system in the development and manifestations of SLE, Curr. Opin. Rheumatol. 24 (2012) 499–505.
[20] D.H. Kono, R. Baccala, A.N. Theofilopoulos, TLRs and interferons: a central paradigm in autoimmunity, Curr. Opin. Immunol. 25 (2013) 720–727.
[21] T. Weichhart, M. Hengstschlager, M. Linke, Regulation of innate immune cell function by mTOR, Nat. Rev. Immunol. 15 (2015) 599–614.
[22] A. Perl, mTOR activation is a biomarker and a central pathway to autoimmune disorders, cancer, obesity, and aging, Ann. N. Y. Acad. Sci. 1346 (2015) 33–44.
[23] Z. Oaks, A. Perl, Metabolic control of the epigenome in systemic Lupus erythematosus, Autoimmunity 47 (2014) 256–264.
[24] M. Zhao, J. Wang, W. Liao, D. Li, M. Li, H. Wu, Y. Zhang, M.E. Gershwin, Q. Lu, Increased 5-hydroxymethylcytosine in CD4(+) T cells in systemic lupus erythematosus, J. Autoimmun. 69 (2016) 64–73.
[25] T. Koga, C.M. Hedrich, M. Mizui, N. Yoshida, K. Otomo, L.A. Lieberman, T. Rauen, J.C. Crispin, G.C. Tsokos, CaMK4-dependent activation of AKT/mTOR and CREM-alpha underlies autoimmunity-associated Th17 imbalance, J. Clin. Invest. 124 (2014) 2234–2245.
[26] S. Kshirsagar, M. Riedl, H. Billing, B. Tonshoff, S. Thangavadivel, C. Steuber, H. Staude, G. Wechselberger, M. Edelbauer, Akt-dependent enhanced migratory capacity of Th17 cells from children with lupus nephritis, J. Immunol. 193 (2014) 4895–4903.
[27] Z.W. Lai, R. Borsuk, A. Shadakshari, J. Yu, M. Dawood, R. Garcia, L. Francis, H. Tily, A. Bartos, S.V. Faraone, P. Phillips, A. Perl, Mechanistic target of rapamycin activation triggers IL-4 production and necrotic death of double-negative T cells in patients with systemic lupus erythematosus, J. Immunol. 191 (2013) 2236–2246.
[28] A. Perl, R. Hanczko, Z.W. Lai, Z. Oaks, R. Kelly, R. Borsuk, J.M. Asara, P.E. Phillips, Comprehensive metabolome analyses reveal N-acetylcysteine-responsive accumulation of kynurenine in systemic lupus erythematosus: implications for activation of the mechanistic target of rapamycin, Metabolomics 11 (2015) 1157–1174.
[29] T. Kobayashi, S. Shimabukuro-Demoto, R. Yoshida-Sugitani, K. Furuyama-Tanaka, H. Karyu, Y. Sugiura, Y. Shimizu, T. Hosaka, M. Goto, N. Kato, T. Okamura, M. Suematsu, S. Yokoyama, N. Toyama-Sorimachi, The histidine transporter SLC15A4 coordinates mTOR-dependent inflammatory responses and pathogenic antibody production, Immunity 41 (2014) 375–388.
[30] Z. Gu, W. Tan, J. Ji, G. Feng, Y. Meng, Z. Da, G. Guo, Y. Xia, X. Zhu, G. Shi, C. Cheng, Rapamycin reverses the senescent phenotype and improves immunoregulation of mesenchymal stem cells from MRL/lpr mice and systemic lupus erythematosus patients through inhibition of the mTOR signaling pathway, Aging 8 (2016) 1102–1114.
[31] Z. Oaks, T. Winans, T. Caza, D. Fernandez, Y. Liu, S.K. Landas, K. Banki, A. Perl, Mitochondrial dysfunction in the liver and antiphospholipid antibody production precede disease onset and respond to rapamycin in lupus-prone mice, Arthritis Rheumatol. 68 (2016) 2728–2739.
[32] M.B. Buechler, H.M. Akilesh, J.A. Hamerman, Cutting edge: direct sensing of TLR7 ligands and type I IFN by the common myeloid progenitor promotes mTOR/PI3K-dependent emergency myelopoiesis, J. Immunol. 197 (2016) 2577–2582.
[33] P.W.F. Karmaus, A.A. Herrada, C. Guy, Critical Roles of mTORC1 Signaling and Metabolic Reprogramming for M-CSF-mediated Myelopoiesis, vol. 214, (2017), pp. 2629–2647.
[34] T. Okada, A.Y. Lee, L.X. Qin, N. Agaram, T. Mimae, Y. Shen, R. O'Connor, M.A. Lopez-Lago, A. Craig, M.L. Miller, P. Agius, E. Molinelli, N.D. Socci, A.M. Crago, F. Shima, C. Sander, S. Singer, Integrin-alpha10 dependency identifies RAC and RICTOR as therapeutic targets in high-grade myxofibrosarcoma, Cancer Discov. 6 (2016) 1148–1165.
[35] P.Y. Lee, J.S. Weinstein, D.C. Nacionales, P.O. Scumpia, Y. Li, E. Butfiloski, N. van Rooijen, L. Moldawer, M. Satoh, W.H. Reeves, A novel type I IFN-producing cell subset in murine lupus, J. Immunol. 180 (2008) 5101–5108.
[36] P.Y. Lee, Y. Kumagai, Y. Li, O. Takeuchi, H. Yoshida, J. Weinstein, E.S. Kellner, D. Nacionales, T. Barker, K. Kelly-Scumpia, N. van Rooijen, H. Kumar, T. Kawai, M. Satoh, S. Akira, W.H. Reeves, TLR7-dependent and FcgammaR-independent production of type I interferon in experimental mouse lupus, J. Exp. Med. 205 (2008) 2995–3006.
[37] H. Ma, S. Wan, C.Q. Xia, Immunosuppressive CD11b + Ly6Chi monocytes in pristane-induced lupus mouse model, J. Leukoc. Biol. 99 (2016) 1121–1129.
[38] F. Wang, B. Li, N. Schall, M. Wilhelm, S. Muller, Assessing autophagy in mouse models and patients with systemic autoimmune diseases, Cell 6 (2017).
[39] D. Perry, A. Sang, Y. Yin, Y.Y. Zheng, L. Morel, Murine models of systemic lupus erythematosus, J Biomed Biotechnol 2011 (2011) 271694.
[40] R.J. Flynn, CD95 and the MRL-lpr mouse model, Methods Mol. Biol. 1557 (2017) 219–228.

[41] M.N. Martina, S. Noel, A. Saxena, H. Rabb, A.R. Hamad, Double negative (DN) alphabeta T cells: misperception and overdue recognition, Immunol. Cell Biol. 93 (2015) 305–310.
[42] D.M. Hammond, P.S. Nagarkatti, L.R. Gote, A. Seth, M.R. Hassuneh, M. Nagarkatti, Double-negative T cells from MRL-lpr/lpr mice mediate cytolytic activity when triggered through adhesion molecules and constitutively express perforin gene, J. Exp. Med. 178 (1993) 2225–2230.
[43] M. Sade-Feldman, J. Kanterman, E. Ish-Shalom, M. Elnekave, E. Horwitz, M. Baniyash, Tumor necrosis factor-alpha blocks differentiation and enhances suppressive activity of immature myeloid cells during chronic inflammation, Immunity 38 (2013) 541–554.
[44] S.R. Christensen, J. Shupe, K. Nickerson, M. Kashgarian, R.A. Flavell, M.J. Shlomchik, Toll-like receptor 7 and TLR9 dictate autoantibody specificity and have opposing inflammatory and regulatory roles in a murine model of lupus, Immunity 25 (2006) 417–428.
[45] R. Fukui, A. Kanno, K. Miyake, Type I IFN contributes to the phenotype of Unc93b1D34A/D34A mice by regulating TLR7 expression in B cells and dendritic cells, J. Immunol. 196 (2016) 416–427.
[46] I.B. Bekeredjian-Ding, M. Wagner, V. Hornung, T. Giese, M. Schnurr, S. Endres, G. Hartmann, Plasmacytoid dendritic cells control TLR7 sensitivity of naive B cells via type I IFN, J. Immunol. 174 (2005) 4043–4050.
[47] N.M. Green, A. Laws, K. Kiefer, L. Busconi, Y.M. Kim, M.M. Brinkmann, E.H. Trail, K. Yasuda, S.R. Christensen, M.J. Shlomchik, S. Vogel, J.H. Connor, H. Ploegh, D. Eilat, I.R. Rifkin, J.M. van Seventer, A. Marshak-Rothstein, Murine B cell response to TLR7 ligands depends on an IFN-beta feedback loop, J. Immunol. 183 (2009) 1569–1576.
[48] F.J. Barrat, K.B. Elkon, K.A. Fitzgerald, Importance of nucleic acid recognition in inflammation and autoimmunity, Annu. Rev. Med. 67 (2016) 323–336.
[49] G.S. Garcia-Romo, S. Caielli, B. Vega, J. Connolly, F. Allantaz, Z. Xu, M. Punaro, J. Baisch, C. Guiducci, R.L. Coffman, F.J. Barrat, J. Banchereau, V. Pascual, Netting neutrophils are major inducers of type I IFN production in pediatric systemic lupus erythematosus, Sci. Transl. Med. 3 (2011) 73ra20.
[50] L. Ronnblom, M.L. Eloranta, G.V. Alm, The type I interferon system in systemic lupus erythematosus, Arthritis Rheum. 54 (2006) 408–420.
[51] F.J. Barrat, T. Meeker, J. Gregorio, J.H. Chan, S. Uematsu, S. Akira, B. Chang, O. Duramad, R.L. Coffman, Nucleic acids of mammalian origin can act as endogenous ligands for Toll-like receptors and may promote systemic lupus erythematosus, J. Exp. Med. 202 (2005) 1131–1139.
[52] T.K. Means, E. Latz, F. Hayashi, M.R. Murali, D.T. Golenbock, A.D. Luster, Human lupus autoantibody-DNA complexes activate DCs through cooperation of CD32 and TLR9, J. Clin. Invest. 115 (2005) 407–417.
[53] R. Bethunaickan, R. Sahu, A. Davidson, Analysis of renal mononuclear phagocytes in murine models of SLE, Methods Mol. Biol. 900 (2012) 207–232.
[54] L. Schiffer, R. Bethunaickan, M. Ramanujam, W. Huang, M. Schiffer, H. Tao, M.P. Madaio, E.P. Bottinger, A. Davidson, Activated renal macrophages are markers of disease onset and disease remission in lupus nephritis, J. Immunol. 180 (2008) 1938–1947.
[55] R. Sahu, R. Bethunaickan, S. Singh, A. Davidson, Structure and function of renal macrophages and dendritic cells from lupus-prone mice, Arthritis Rheumatol. 66 (2014) 1596–1607.
[56] F. Veglia, M. Perego, Myeloid-derived Suppressor Cells Coming of Age, vol. 19, (2018), pp. 108–119.
[57] S. Chen, L. Wang, J. Fan, C. Ye, D. Dominguez, Y. Zhang, T.J. Curiel, D. Fang, T.M. Kuzel, B. Zhang, Host miR155 promotes tumor growth through a myeloid-derived suppressor cell-dependent mechanism, Cancer Res. 75 (2015) 519–531.
[58] Y. Song, H. Dou, X. Li, X. Zhao, Y. Li, D. Liu, J. Ji, F. Liu, L. Ding, Y. Ni, Y. Hou, Exosomal miR-146a contributes to the enhanced therapeutic efficacy of interleukin-1beta-primed mesenchymal stem cells against sepsis, Stem Cells 35 (2017) 1208–1221.